Title: Articular cartilage corefucosylation regulates tissue resilience in osteoarthritis

Short title: Articular cartilage corefucosylation and tissue resilience in OA

Kentaro Homan[1], Tomohiro Onodera[1]*, Hisatoshi Hanamatsu[2], Jun-ichi Furukawa[1, 2], Daisuke Momma[3], Masatake Matsuoka[1], Norimasa Iwasaki[1]

[1] Department of Orthopaedic Surgery, Faculty of Medicine and Graduate School of Medicine, Hokkaido University, Kita 15, Nishi 7, Kita-ku, Sapporo 060-8638, Japan

[2] Institute for Glyco-core Research (iGCORE), Nagoya University, Nagoya 464-8601, Japan

[3] Center for Sports Medicine, Hokkaido University Hospital, Kita 14, Nishi 5, Sapporo 060-8638, Japan.

*Corresponding author: Tomohiro Onodera

Department of Orthopaedic Surgery, Faculty of Medicine and Graduate School of Medicine

Hokkaido University, Kita 15, Nishi 7, Kita-ku, Sapporo 060-8638, Japan

Telephone: +81-11-706-2111

Email: tomozou@med.hokudai.ac.jp

Abstract

This study aimed to investigate the glycan structural changes that occur before histological degeneration in osteoarthritis (OA) and to determine the mechanism by which these glycan conformational changes affect cartilage degeneration. An OA model was established in rabbits using mannosidase injection, which reduced high-mannose type N-glycans and led to cartilage degeneration. Further analysis of glycome in human OA cartilage identified specific corefucosylated N-glycan expression patterns. Inhibition of N-glycan corefucosylation resulted in unrecoverable cartilage degeneration, while cartilage-specific blocking of corefucosylation led to accelerated development of aging-associated and instability-induced OA models. We conclude that α1,6 fucosyltransferase is required postnatally to prevent preosteoarthritic deterioration of articular cartilage. These findings provide a novel definition of early OA and identify glyco-phenotypes of OA cartilage, which may distinguish individuals at higher risk of progression.

Keywords: early osteoarthritis, glyco-phenotypes, α1,6 fucosyltransferase, cartilage glycome

INTRODUCTION

Osteoarthritis (OA), a degeneration of joint components, such as proteoglycans (PGs) and collagen, destroys cartilage and impairs joint function (1). The global prevalence of OA is estimated to be >500 million, which is a significant socioeconomic burden (2). Therefore, preventive measures must be implemented to reduce the future disease burden and disability. Once the cartilage is destroyed, it cannot be repaired homogeneously and progresses irreversibly thereafter (3, 4). Since articular cartilage has no blood vessels and is not innervated, it is difficult for symptoms to appear. By the time clinical symptoms appear, the condition is often already considerably advanced (5). Therefore, from a preventive

46 perspective, it is necessary to define and detect "pre-OA," the stage before the onset of early
47 OA (6, 7). Pre-OA is a knee with no pain, no motor function problems, and no arthroscopic or
48 structural changes on radiography, only emerging cellular effects. Despite many studies, there
49 is no gold standard for OA biomarkers (8). It is important to characterize the disease state
50 before OA to shift the paradigm from mitigation to late-onset disease prevention.
51 In the very early stages of OA, before cartilage matrix degeneration, cartilage destruction by
52 enzymatic processes that degrade glycoproteins, PGs, and collagen, in that order, is underway
53 (9). Collagenolytic activity is largely unchanged on intact articular surfaces (10, 11), and
54 glycoprotein degradation is thought to be an early transient event in the enzymatic process of
55 cartilage destruction because hexose degradation of glycoproteins promotes degradation of
56 the protein portion of the molecule by proteinases (12). Additionally, cartilage damage is
57 reversible if type 2 collagen breakdown is mild (13). Structural change analysis in
58 glycoproteins is necessary for the early stages of OA but has not yet been performed
59 sufficiently.
60 Matsuhashi *et al*.'s study showed that structural changes in N-glycans occurred in
61 degenerated cartilage in a rabbit OA model before tissue changes occurred (14). Urita *et al*.
62 demonstrated that these N-glycans in degenerated mice and human cartilage are high-
63 mannose type N-glycans (15). Furthermore, among several glycosidases, mannosidase
64 activity was very high in OA joints, and its activity was high before the progression of
65 cartilage fibrosis (16). This suggests that high-mannose type N-glycan plays an important
66 role in OA pathogenesis. However, whether changes in the glycan structure are involved in
67 OA pathogenesis is unclear.
68 This study analyzed the glycan structural changes that preceded OA degeneration and
69 elucidated the mechanism of glycan structural changes in cartilage degeneration. For this
70 purpose, the effects of mannosidase, a specific degrading enzyme of high-mannose type N-

glycans associated with OA, on cartilage tissues and its molecular mechanisms were analyzed.

RESULTS

Mannosidase injection caused early OA-like change in vivo

A decrease in Safranin O staining in the right femoral condyle of the α-mannosidase-injected knee after 4 weeks was observed (Fig. 1A, B). Terminal deoxynucleotidyl transferase dUTP nick end labeling (TUNEL) staining was enhanced in the superficial layer compared with that in control. Articular cartilage chondrocytes exposed to α-mannosidase were not arranged in columns in the middle zone. The surfaces of each group were smooth and had a good macroscopic appearance (Fig. 1C). None of the groups showed a decrease in type 2 collagen staining, and the orientation was maintained (Fig. 1D). To achieve optimal activity, the pH range of 4 to 5 is ideal for mannosidase. In a physiological saline solution with a pH of 7 and a concentration of 100 μg/ml, it exhibited specific activity. Nevertheless, at a concentration of 1.0 μg/ml, this activity was no longer present (S1 Figure). The mean histological score of the α-mannosidase group was 0.83, indicating mild OA (Fig. 1E). The control group was unchanged. Cartilage degeneration during intermittent intra-articular administration of mannosidase was reversed upon discontinuation (Fig. 1F).

Depletion of high-mannose type N-glycans in chondrocytes leads to cartilage degradation ex vivo

To quantify the degeneration and resilience promoted by the injection of α-mannosidase, the cultured cartilage was harvested at different time points (Fig. 2A). Concanavalin A (Con A) reactivity declined in articular cartilage treated with α-mannosidase (Fig. 2B). The application of α-mannosidase stimulated the release of PG from cultured cartilage in

association with extracellular matrix degradation (Fig. 2C) and showed significantly higher spontaneous nitric oxide (NO) release than the control over time (Fig. 2F). Mannosidase-exposed cartilage showed an increase in TUNEL-positive cells in chondrocytes in the deep zone and type 10 collagen-positive cells in superficial chondrocytes; however, these changes did not occur in cytokine-stimulated cartilage (S2 Figure). Mannosidase exposure increased *Adamts5* expression and suppressed *Mmp13* expression and anabolic factors (Fig. 3E). In the articular cartilage that was exposed to freeze-thaw treatment before culture, no differences in PG loss were observed between the α-mannosidase-stimulated cartilage and non-stimulated cartilage (Fig. 2E). Excluding mannosidase loading, PG leakage and Safranin O staining were restored (Fig. 2D), but Con A staining loss was not. Sialidase addition did not cause PG leakage or NO production (S3 Figure), and the aggrecan lost in the catabolic phase was not replenished in the subsequent anabolic phase.

Corefucosylated N-glycan was formed in resilient cartilage

Glycoblotting analysis revealed a significant difference in the N-glycan profiles (Fig. 3A and S1 Table). Plotting m/z after mannosidase exposure against m/z before mannosidase exposure demonstrated that only N-glycans were affected by enzyme dissociation from the y = x line (Fig. 3B, S2 Table). In both denatured and reverted cartilages, Man8-9GlcNAc2 was decreased, and Man5-6GlcNAc2 was increased by the action of mannosidase, which has a high specificity for the terminal mannosidic residues of glycans (Fig. 3C, D). In contrast, corefucosylated N-glycans, which were formed in the same biosynthesis pathway, were also found (Fig. 3D). Similarly, the N-glycan profiles of isolated chondrocytes showed the presence of this corefucosylated structure (S4 Figure). The expression of *Fut8*, the only enzyme involved in corefucosylation, increased significantly in mannosidase-treated cartilage (Fig. 3E).

Deficiency of corefucosylated glycans in articular cartilage inhibits recovery from cartilage damage and promotes cartilage degeneration

We first examined whether the absence of core fucose affects the resilience of cartilage degeneration. Mice lacking *Fut8* exhibited severe growth retardation and died shortly after birth. Therefore, we decided to generate *Fut8* conditional knockout (cKO) mice (Fig. 4A, B). The tissue specificity of recombination was confirmed by polymerase chain reaction (PCR) analysis of mouse genomic DNA that detected either the intact $Fut8^{loxP}$ allele or the Cre-recombined $Fut8^{\Delta}$ allele in repeated crosses; N-glycan analysis of cartilage demonstrated the loss of corefucosylated sugar chains (Fig. 4C). The proportion of high-mannose type N-glycan content was unchanged in cartilage lacking the *Fut8* gene (S5 Figure). Next, we used real-time (RT)-PCR to determine relative *Fut8* messenger (m)-RNA levels in the cartilage of Col2-$Fut8^{-/-}$ mice and their wild-type (WT) littermates ($Fut8^{loxP/loxP}$). Real-time polymerase chain reaction (RT-PCR) analysis showed that *Fut8* mRNA expression was reduced by >99% in the articular cartilage of Col2-$Fut8^{-/-}$ mice compared to that in their WT littermates ($P < 0.01$; n = 3 mice per group) (Fig. 4D). Chondrocyte-surface corefucosylation levels were analyzed by lectin staining using *Pholiota squarrosa* lectin (PhoSL), which specifically recognizes α1-6 core fucose (17). PhoSL lectin staining was completely absent in the articular cartilage of *Fut8* cKO mice, in contrast to the positive staining observed in *Fut8* flox mice under physiological conditions (Fig. 4E). Enzymatic degradation of high-mannose type N-glycans on the cartilage in *Fut8*-deficient mice exacerbated cartilage degeneration (Fig. 4E, F). In addition, reversible matrix repair by enzyme removal observed in control cartilage was not observed in *Fut8*-deficient cartilage explant cultures.

Loss of corefucosylated glycans in articular cartilage leads to premature OA

Col2-*Fut8*$^{-/-}$ mice developed and grew normally without major organ abnormalities of major organs and could not be distinguished from their WT littermates. The whole skeletons of newborn mice stained with alcian blue and alizarin red did not differ in appearance between the genotypes (Fig. 5A). Col2-*Fut8*$^{-/-}$ mice showed a lower body weight than their WT littermates, as indicated by the growth curve (Fig. 5B). We analyzed the development of instability-induced OA changes in *Fut8*$^{loxP/loxP}$ and *Fut8* cKO mice. Sham operations produced no significant changes in OA in either mouse genotype. Eight weeks after instability-inducing surgery, the joints of WT mice developed changes in OA, such as cartilage erosion and a reduction in Safranin O staining and chondrocyte number. Deletion of FUT8 results in more severe changes in OA. In the joints of *Fut8* cKO mice, 8 weeks after surgery, the noncalcified zone (upper layer above the tidemark) was almost completely lost. The number of chondrocytes was significantly reduced (Fig. 5C). Quantitative assessment using the OA Research Society International (OARSI) score supported these histological findings (difference: -2.900; *Fut8*$^{flox/flox}$/destabilization of the medial meniscus (DMM) versus *Col2a1-Cre*; *Fut8*$^{flox/flox}$/DMM, 95% confidence interval [CI] for the difference: -5.027 to -0.7734) (Fig. 5D). Changes in OA progressed earlier in the aging models of *Fut8*-deficient mice than in control mice (WT and floxed mice). The mice were followed up until 15 months of age to assess the spontaneous development of OA with aging (Fig. 5E). There were no apparent changes of OA in the knee joints of either mouse genotype at 3 months of age (Fig. 5F). At 4 months of age, significant changes in OA were detected in the knee joints of the *Fut8* cKO mice. The cartilage surface integrity was no longer maintained at 9 months. These OA changes progressed more in *Fut8* cKO mice than in their WT littermates at 15 months. These histological findings were quantitatively confirmed by the Osteoarthritis Research Society International (OARSI) scores (difference: -2.000; WT versus *Col2a1-Cre; Fut8*$^{flox/flox}$,

95% CI for the difference: -3.723 to -0.2771 at 4 months, difference: -2.700; WT versus *Col2a1-Cre; Fut8*$^{flox/flox}$, 95% CI for the difference: -4.423 to -0.9771 at 9 months, and difference: -6.700; WT versus *Col2a1-Cre; Fut8*$^{flox/flox}$, 95% CI for the difference: -8.423 to -4.977 at 15 months).

Altered glycosylation of human OA cartilage based on comprehensive glycan analysis

Total glycome profiling of human OA cartilage is shown in Fig. 6A and S3 Table. The amount of high-mannose type N-glycan was significantly decreased, the same as previously reported in OA cartilages (Fig. 6A) (15). Focusing on fucosylation, most of the complex/hybrid type glycans were modified with fucose. The fucosylation that occurs at the innermost N-acetylglucosamine (GlcNAc) of N-glycans could be recognized with a lectin from the mushroom Pholiota squarrosa (PhoSL) and was able to detect the expression of the corefucose structure. Therefore, we suspected that the stainability of PhoSL is increased in OA cartilage. As expected, the PhoSL staining of OA cartilage was significantly increased relative to that of a healthy control (Fig. 6B). We performed principal component analysis (PCA) on 1110 glycomic data, discriminating OA from healthy cartilages along the first principal component (PC1) axis (Fig. 6C). Hierarchical cluster analysis showed that clades containing corefucosylated glycans were clustered (Fig. 6D), and N-13 ((Hex)1 (HexNAc)1 (Fuc)1 + (Man)3(GlcNAc)2) has the largest squared correlation with its cluster component.

DISCUSSION

To test the hypothesis that structural changes in high-mannose type N-glycans may induce OA, we tested the effect of mannosidase loading on the structure of high-mannose type N-glycans. Consequently, modifying the structure of high-mannose type N-glycans by mannosidase loading induced OA-like histological alterations. Furthermore, the OA-like

changes induced by mannosidase were recovered by enzyme removal. These results suggest that structural alterations of high-mannose type N-glycans lead to OA-like histological changes in articular cartilage but do not necessarily cause the pathogenesis of eventual OA. Subsequently, glycoblotting analysis revealed that core-fucose-containing glycans underwent complementary structural alterations per high-mannose type N-glycans. This suggests that the structural change of core-fucose-containing glycans may have some compensatory mechanism for OA-like alterations caused by the structural change of high-mannose type N-glycans. Furthermore, under the regulation of *Fut8* expression, which regulates the synthesis of core fucose, mannosidase was found to induce irreversible OA. These results provide the first evidence that structural alterations in glycans in the articular cartilage regulate eventual OA development.

Two key targets of cartilage degeneration during OA are type II collagen, a major substrate of matrix metalloproteinase (MMP)-13 (18), and aggrecan, a PG with glycosaminoglycan side chains of chondroitin and keratin sulfate (19, 20). The degradation of non-collagenous molecules, such as aggrecan, occurs before the degradation of type II collagen in the early stages of OA (20, 21). The histological analysis in this study revealed that the alteration in the structure of high-mannose type N-glycans resulted in a decrease in Safranin O staining (a decrease in glycosaminoglycans and/or PGs), whereas there was no change in collagen staining. These findings are consistent with alterations in the early stages of OA. Furthermore, we observed that removing mannosidase could cause PG loss to the control level. Karsdal *et al.* demonstrated that articular cartilage degradation is reversible in the presence of aggrecanase and concluded that the repair ability is not impaired before the degradation of aggrecan and type II collagen by MMPs (22). Reimann *et al.* observed that the glycosaminoglycans loss in articular cartilage is reversible and an early sign of OA before the "state of no return." (23) The present results are consistent with findings of previous reports

on early OA and suggest that the mannosidase-loaded model can be considered an early OA-like alteration.

Since the structural change in high-mannose type N-glycans alone did not cause irreversible OA, we investigated other regulatory mechanisms related to high-mannose type N-glycans that could induce irreversible OA. The expression of corefucosylated N-glycans on a series of biosynthetic pathways was upregulated with structural changes in high-mannose type N-glycans. FUT8 is known to corefucosylate small oligomannose N-glycans (Man4-Man5GlcNAc2) but not large oligomannose N-glycans, such as Man8-Man9GlcNAc2 (24). This suggests that small oligomannose N-glycans trimmed by mannosidase could activate *Fut8*. *Fut8* is also upregulated in human OA chondrocytes (25, 26), and increased expression of these corefucosylated N-glycans has been observed during late chondrocyte differentiation (27). These findings suggested that these structural changes are related to OA-related glycosylation.

To clarify the relationship between the alteration of corefucosylated N-glycans and cartilage degeneration, *Fut8* cKO mice were used. Since the results of the ex vivo freeze-thaw model showed that cartilage degeneration was induced by changes in the glycan structure of chondrocytes, we used chondrocyte-specific KO mice. As a result, the reversibility of the cartilage degeneration model was diminished. This finding suggests that *Fut8*-mediated corefucosylation in chondrocytes plays a function in promoting glycan repair. Furthermore, to directly determine whether *Fut8* was involved in the inhibition of OA progression, an aging model was investigated. The results showed that conditional KO of *Fut8* in chondrocytes hastened the onset of OA. This suggests that cartilage corefucosylation associated with FUT8 plays a protective role against the attenuation of type II collagen in the OA process.

Finally, the expression of α1,6-linked core fucose on N-glycans in human cartilage is associated with OA, and corefucosylation was found to be one of the characteristics in OA

cartilage. Total cellular glycome analysis, including N- and O-linked glycans derived from glycoproteins, GSL-glycans, GAGs, and fOSs, is informative for analyzing cell-specific characteristics (28–30). Glycome profiling enabled the detection of corefucosylated N-glycans by sequential clustering of degenerated cartilage characteristics. Core fucose deficient mice generated by ablating the α1,6 fucosyltransferase enzyme, FUT8, were reported to have suppressed phosphorylation of Smad and increased expression of MMPs (matrix metalloproteinases) due to decreased binding of TGF-β ligand caused by the lack of core fucose addition to the TGF-β type II receptor (31, 32). The present study shows that treatment of cartilage with mannosidase caused corefucosylation, suppression of *Mmp13*, and increased expression of *Tgf-β*. Moreover, treatment of FUT8-knockout cartilage with mannosidase resulted in the suppression of *Tgf-β* expression and increased *Mmp13* expression. These results suggest that corefucosylation following the loss of high-mannose type N-glycans may provide chondroprotective effects via the TGF-β signaling pathway, which may have been lost by FUT8-knockout.

One limitation of this study was that we did not have access to cartilage samples from immediately before the onset of OA; thus, we do not know the expression of Fut8 in human cartilage in the early stage of OA onset and its influence on extracellular matrix degradation under homeostatic conditions. Obtaining cartilage specimens continues to be challenging, especially for those with early stages of OA.

In summary, we show for the first time a key role of FUT8 and glycan-dependent signaling mediators in extracellular matrix resilience associated with cartilage corefucosylation during early OA.

METHODS

Intra-articular injection of α-mannosidase in the knee

Japanese White rabbits weighing 3.10 ± 0.15 kg purchased from a professional breeder (Japan SLC Inc., Hamamatsu, Japan) were used for this study according to established ethical guidelines approved by the local animal care committee. Animals were anesthetized with 10 mg/kg of intravenous ketamine, followed by isoflurane in oxygen gas. Both knees in each rabbit were shaved, prepared, and draped in a sterile fashion. α-Mannosidase from Canavalia ensiformis (Jack bean) (Sigma, St Louis, MO, USA) was dissolved in saline. Five hundred microliter volumes containing 1.9 units per ml (0.05 mg) of mannosidase solution were injected into the joint cavity of the right knee. α-Mannosidase from Canavalia ensiformis (Jack bean) has been widely used as a tool for glycan analysis, which has a high specificity towards terminal mannosidic residues of glycans and participates in mannose trimming reactions (33). The measurement of its performance in a saline solution was evaluated using the QuantiChrom α-Mannosidase Assay Kit (BioAssay Systems, Hayward, CA, USA). This colorimetric assay uses 4-nitrophenyl-α-d-mannopyranoside as a substrate to identify the generation of 4-nitrophenol. The following doses of α-Mannosidase were administered: 0.5 ml at 0.01 μg/ml, 1.0 μg/ml, or 100 μg/ml. Simultaneously, the contralateral knee joint received an equal volume of saline solution. Each joint was injected once or four times in alternate weeks. The animals were euthanized at 4 and 16 weeks postoperatively. Each section of the knee joint was stained with hematoxylin and eosin or Safranin O/fast green, as well as with immunohistochemical staining for type II collagen and TUNEL. Two investigators quantified the OA severity using the OARSI scoring method.

Evaluation of collagen orientation by a polarized light microscope

To evaluate the collagen orientation of the repaired tissue at 16 weeks postoperatively, a

supplemental evaluation using a polarized light microscope (PLM) (ECLIPSE E600 POL; Nikon, Tokyo, Japan) was conducted (34). This evaluation was performed on HE-stained sections from each group. Two cross polarizers were used so that highly ordered collagen perpendicular to the articular surface appeared bright, while collagen that was not ordered (nonbirefringent) appeared dark. The contrast of fibrils more parallel to the articular surface was darker than collagen oriented perpendicular to the articular surface. To observe the predominant direction of the birefringent regions and confirm the lack of orientation in the nonbirefringent regions, the sections were rotated at 0°, 45°, and 90° for the fixed filters. Microscopic images were acquired using a digital camera (DS-5M-L1, Nikon, Tokyo, Japan). Each sample was examined independently by an experienced PLM user.

Ex vivo analysis of deletion of high-mannose type N-glycan in cartilage

According to the established ethical guidelines approved by the local animal care committee, cartilage catabolism was analyzed by culturing femoral head cartilage of 4-week-old C57BL6 male mice with α-mannosidase (1.9 U/mL) ex vivo (35, 36). Mannosidase was removed on day 3, and organ culture was continued until day 6. To evaluate cartilage degradation, quantification of PG release from cartilage explants was performed using the dimethylmethylene blue assay (36, 37) and exposure to sialidase (1.9 U/mL) and interleukin-1 beta (Cat #. 300-01A; BioLegend, San Diego, CA, USA) (10 ng/mL) was also used as another control. The NO concentration in the culture medium was measured using the Griess reagent system (Promega, Tokyo, Japan). To determine the direct effects of mannosidase on the matrix, some cartilage explants were subjected to freeze-thaw cycles in liquid nitrogen to destroy chondrocytes present in the superficial layer of the cartilage (22, 38). After the procedure, the cells were replaced with the same culture medium described above. Each tissue sample was stained with Safranin O. Lectin staining with Con A (Wako Pure Chemical

Industries, Richmond, VA, USA) and PhoSL (J-Oil Mills Inc., Tokyo, Japan) was used to detect the high-mannose type N-glycans. Staining was performed using the ABC Kit (Vector Labs, Burlingame, CA, USA), and the sections were counterstained with HE.

RNA extraction and quantitative RT-PCR analysis

Total RNA was extracted from the samples using an RNeasy Mini Kit (Qiagen, Hilden, Germany). For complementary DNA synthesis, 1.0 μg of RNA was reverse transcribed using random hexamer primers (Promega, Tokyo, Japan) and ImProm II reverse transcriptase (Promega). Quantitative RT-PCR was performed using a Thermal Cycler Dice Real Time System II (Takara Bio Inc., Otsu, Japan) and SYBR Premix Ex Taq II (Takara, Shiga, Japan) with gene-specific primers (S4 Table) in 15 μl of the mixture, following the manufacturer's instructions. Quantitative data were normalized using peptidylprolyl isomerase A as an endogenous reference gene and were calculated using the ΔΔCt method (39).

Generation of *Fut8*$^{loxp/loxp}$*Col2a1-Cre* cKO mice

Fut8$^{loxp/loxp}$ mice were provided by Tohoku Pharmaceutical University (Sendai, Japan). To interrupt the synthesis of corefucosylated N-glycans in cartilage, we generated mice with knockout of the chondrocyte-specific *Fut8* gene (Col2-*Fut8*$^{-/-}$ mice) by crossing *Fut8*$^{loxp/lox}$ mice with Col2a1-Cre–transgenic mice (40), in which Cre recombinase is expressed specifically in chondrocytes under the Col2a1 promoter. Transgenic mice carrying the Col2a1-Cre transgene (strain B6; SJL-Tg [Col2a1-Cre] 1Bhr/J; stock number 003554) were obtained from the Jackson Laboratory (Bar Harbor, ME, USA). Homozygous *Fut8*$^{loxp/loxp}$ mice were bred with *Col2a1-Cre* mice, and offspring with the genotype *Fut8*$^{loxp/+}$ *Col2a1-Cre* were bred with *Fut8*$^{loxp/loxp}$ mice to obtain the *Fut8*$^{loxp/loxp}$*Col2a1-Cre* cKO experimental group and *Fut8*$^{loxp/loxp}$ (flox) littermate controls. All animals were maintained at Hokkaido

University under the regulations of the Institutional Animal Care and Use Committee.

Skeletal examination

To observe the skeletal systems, whole skeletons of WT and cKO littermates were stained with alcian blue and alizarin red, as previously described (41, 42). The newborns were skinned, eviscerated, and fixed in 95% ethanol. Intact skeletons were stained with 150 mg/ml of alcian blue 8GX in 75% (vol/vol) ethanol/20% acetic acid for 24–48 hours, and excess tissues were removed by 1–2% KOH digestion for 2–3 days. The skeletal preparations were stained with 75 mg/ml of alizarin red S in 1% KOH for 24 hours and cleared in graded glycerol solutions (43).

Instability-induced OA model

An OA model was created in 10-week-old mice by destabilizing the knee joint as previously described (44). With the mice under general anesthesia, we destabilized the right knee joint by transection of the medial collateral ligament and removing the cranial half of the medial meniscus using a microsurgical technique (DMM). A sham operation was performed on the left knee joint using the same approach, without ligament transection and meniscectomy. For histological assessment, the mice were sacrificed, and the entire knee joint was dissected 8 weeks postoperatively.

Age-associated OA model

At 3, 4, 9, and 15 months of age, the mice were sacrificed, and their entire knee joints were dissected to assess the spontaneous development of OA as a model of age-associated OA (44, 45).

368 **Human Cartilage Preparation**

369 Acquisition and use of patient tissues were approved by the institutional review board (IRB)
370 of Hokkaido University (approval number: 014-0144), and informed consent was obtained in
371 advance. Samples were from patients undergoing total knee arthroplasty for clinically and
372 radiologically diagnosed OA (n=5; age range 61–84 years, mean 72.4; male: female ratio
373 1:4). Age-matched control articular cartilage was from patients undergoing total hip
374 arthroplasty for femoral neck fracture with no history of joint disease (n=5; age range 45–88
375 years, mean 61.2 years; male: female ratio 3:2). Each cartilage specimen was evaluated
376 macroscopically by at least two veteran doctors to ensure that it had not suffered damage or
377 degeneration and was treated within 9 hours of harvest in the operating room. Immediately
378 upon receipt, isolated human cartilage was homogenized with a Polytron blender
379 (Kinematica, Luzern, Switzerland), and then cold ethanol was added to separate the protein
380 and lipid fractions.

381

382 **Total cartilage glycomic analysis**

383 N-glycans were released directly using cartilage lysates following deglycosylation by
384 overnight treatment with peptide N-glycanase F (PNGase F, 2U) (Roche, Switzerland). The
385 supernatants containing GSLs and fOSs were dried with a centrifugal evaporator. GSL-
386 glycans were isolated by enzymatic digestion using EGCase I (Takara Bio Inc. Japan),
387 whereas fOSs were recovered from an EGCase I-free fraction (46). Cartilage lysate was
388 delipidated and digested by GAG disaccharides (47). Extracted glycoproteins were subjected
389 to BEP for O-glycan analysis. Detailed procedures and materials are provided elsewhere (48).
390 N-glycans, fOSs, GAGs, and GSL-glycans were subjected to glycoblotting (49). Purified N-
391 glycans, fOSs, O-glycans, and GSL-glycan solutions were mixed with 2,5-dihydrobenzoic
392 acid and subjected to Matrix-assisted laser desorption/ionization-time of flight mass

393 spectrometry (MALDI-TOF MS). 2AB-labeled GAG disaccharides were analyzed by HPLC.
394 The glycan compositions were manually determined by conducting database searches (i.e., a
395 compositional search of the UniCarbKB database (http://www.unicarbkb.org/query) for fOSs
396 and N- and O-glycans and of the SphinGOMAP database (http://www.sphingomap.org/) for
397 GSL-glycans). All previously deposited GSL-glycans in the SphinGOMAP database were
398 extracted and compiled as an in-house database to allow searching by the m/z value and/or
399 composition. The absolute quantification was obtained by comparative analyses between the
400 MS signal areas derived from each glycan and the internal standard.
401
402 **Statistics**
403 All data in this study are presented as the mean standard deviation and were repeated at
404 least three times unless otherwise indicated. Data analysis was performed using GraphPad
405 Prism 9 software version 9.4.1 (GraphPad Software, Inc., San Diego, CA, USA), and the
406 Welch *t*-test/Welch analysis of variance with subsequent use of the Tukey–Kramer multiple
407 comparison tests were used to determine significant differences between the groups. *P*-values
408 <0.05 were considered significant. JMP Pro version 16.2.0 (SAS Institute, Cary, NC, USA)
409 was used to reveal the relationships between each subject of sub glycomes; we performed
410 principal component analysis (PCA) and hierarchical cluster analysis.
411
412 **Study approval**
413 Acquisition and use of patient tissues were approved by the institutional review board (IRB)
414 of Hokkaido University (approval number: 014-0144), and informed consent was obtained in
415 advance. All animal studies were performed according to established ethical guidelines
416 approved by the local animal care committee.
417

418 **Data availability**

419 All data reported in this paper is available from the corresponding author upon request. This
420 paper does not report original code. Any additional information required to reanalyze the data
421 reported in this paper is available from the lead contact upon request.

422

423 **ACKNOWLEDGMENTS**

424 We thank the Iwasaki laboratory members for technical support, J. Gu (Tohoku
425 Pharmaceutical University) for the Flox-α1,6 fucosyltransferase (*Fut8*) mouse, Y. Kobayashi
426 (J-OIL MILLS, Inc.) for PhoSL-lectin. This work was funded by the Japan Society for the
427 Promotion of Science KAKENHI (Grant-in-Aid for Challenging Exploratory Research:
428 funding numbers: 16K15650, 19K22672 [to NI]; Grant-in-Aid for Research (B): funding
429 numbers: 22H03917 [to TO]; and Grant-in-Aid for Early-Career Scientists: funding number:
430 19K18516 [to KH]) and AMED (Grant Number JP22zf01270004h0002 [to NI, TO, KH]).

431

432 **AUTHOR CONTRIBUTIONS**

433 Conceptualization: NI

434 Methodology: KH, TO

435 Investigation: KH, TO, HH, JF, DM, MM, NI

436 Visualization: KH, HH

437 Funding acquisition: KH, NI, TO

438 Project administration: KH, TO, NI

439 Supervision: TO, NI

440 Writing – original draft: KH, TO

441 Writing – review & editing: KH, TO, HH, JF, DM, MM, NI

442

CONFLICT-OF-INTEREST STATEMENT: The authors have declared that no conflict of interest exists.

References

1. Grillet B, et al. Matrix metalloproteinases in arthritis: towards precision medicine. *Nat. Rev. Rheumatol.* [published online ahead of print: May 2023]; doi:10.1038/s41584-023-00966-w
2. Safiri S, et al. Global, regional and national burden of osteoarthritis 1990-2017: a systematic analysis of the Global Burden of Disease Study 2017. *Ann. Rheum. Dis.* 2020;79(6):819–828.
3. Thorstensson CA, et al. Natural course of knee osteoarthritis in middle-aged subjects with knee pain: 12-year follow-up using clinical and radiographic criteria. *Ann. Rheum. Dis.* 2009;68(12):1890–1893.
4. Huey DJ, Hu JC, Athanasiou KA. Unlike bone, cartilage regeneration remains elusive. *Science* 2012;338(6109):917–921.
5. Glyn-Jones S, et al. Osteoarthritis. *Lancet* [published online ahead of print: March 3, 2015]; doi:10.1016/S0140-6736(14)60802-3
6. Chu CR. Defining Pre-Osteoarthritis Is Key to Prevention. *Cartilage* 2016;7(2):204.
7. Mahmoudian A, et al. Early-stage symptomatic osteoarthritis of the knee - time for action. *Nat. Rev. Rheumatol.* 2021;17(10):621–632.
8. Henrotin Y. Osteoarthritis in year 2021: biochemical markers. *Osteoarthritis Cartilage* 2021;S1063-4584(21)00960–2.

9. Vignon E, et al. Screening of degradative enzymes from articular cartilage in experimental osteoarthritis. *Clin. Rheumatol.* 1987;6(2):208–214.

10. Brew CJ, et al. Gene expression in human chondrocytes in late osteoarthritis is changed in both fibrillated and intact cartilage without evidence of generalised chondrocyte hypertrophy. *Ann. Rheum. Dis.* 2010;69(1):234–240.

11. Otero M, et al. Human chondrocyte cultures as models of cartilage-specific gene regulation. *Methods Mol. Biol. Clifton NJ* 2012;806:301–336.

12. Goldring MB. Chondrogenesis, chondrocyte differentiation, and articular cartilage metabolism in health and osteoarthritis. *Ther. Adv. Musculoskelet. Dis.* 2012;4(4):269–285.

13. van Meurs JB, et al. Kinetics of aggrecanase- and metalloproteinase-induced neoepitopes in various stages of cartilage destruction in murine arthritis. *Arthritis Rheum.* 1999;42(6):1128–1139.

14. Matsuhashi T, et al. Alteration of N-glycans related to articular cartilage deterioration after anterior cruciate ligament transection in rabbits. *Osteoarthritis Cartilage* 2008;16(7):772–778.

15. Urita A, et al. Alterations of high-mannose type N-glycosylation in human and mouse osteoarthritis cartilage. *Arthritis Rheum.* 2011;63(11):3428–3438.

16. Snelling S, et al. A gene expression study of normal and damaged cartilage in anteromedial gonarthrosis, a phenotype of osteoarthritis. *Osteoarthr. Cartil. OARS Osteoarthr. Res. Soc.* 2014;22(2):334–343.

17. Kobayashi Y, et al. A novel core fucose-specific lectin from the mushroom Pholiota squarrosa. *J. Biol. Chem.* 2012;287(41):33973–33982.

18. Wu W, et al. Sites of collagenase cleavage and denaturation of type II collagen in aging and osteoarthritic articular cartilage and their relationship to the distribution of matrix metalloproteinase 1 and matrix metalloproteinase 13. *Arthritis Rheum.* 2002;46(8):2087–2094.

19. Song R-H, et al. Aggrecan degradation in human articular cartilage explants is mediated by both ADAMTS-4 and ADAMTS-5. *Arthritis Rheum.* 2007;56(2):575–585.

20. Malfait A-M, et al. Inhibition of ADAM-TS4 and ADAM-TS5 prevents aggrecan degradation in osteoarthritic cartilage. *J. Biol. Chem.* 2002;277(25):22201–22208.

21. Aigner T, et al. Anabolic and catabolic gene expression pattern analysis in normal versus osteoarthritic cartilage using complementary DNA-array technology. *Arthritis Rheum.* 2001;44(12):2777–2789.

22. Karsdal MA, et al. Cartilage degradation is fully reversible in the presence of aggrecanase but not matrix metalloproteinase activity. *Arthritis Res. Ther.* 2008;10(3):R63.

23. Reimann I, Christensen SB, Diemer NH. Observations of reversibility of glycosaminoglycan depletion in articular cartilage. *Clin. Orthop.* 1982;(168):258–264.

24. Yang Q, Wang L-X. Mammalian α-1,6-Fucosyltransferase (FUT8) Is the Sole Enzyme Responsible for the N-Acetylglucosaminyltransferase I-independent Core Fucosylation of High-mannose N-Glycans. *J. Biol. Chem.* 2016;291(21):11064–11071.

25. Toegel S, et al. Glycophenotyping of osteoarthritic cartilage and chondrocytes by RT-qPCR, mass spectrometry, histochemistry with plant/human lectins and lectin localization with a glycoprotein. *Arthritis Res. Ther.* 2013;15(5):R147.

26. Yu H, et al. Characterization of aberrant glycosylation associated with osteoarthritis

based on integrated glycomics methods. *Arthritis Res. Ther.* 2023;25(1):102.

27. Homan K, et al. Alteration of the Total Cellular Glycome during Late Differentiation of Chondrocytes. *Int. J. Mol. Sci.* 2019;20(14):E3546.

28. Fujitani N, et al. Total cellular glycomics allows characterizing cells and streamlining the discovery process for cellular biomarkers. *Proc. Natl. Acad. Sci. U. S. A.* 2013;110(6):2105–2110.

29. Yoshida Y, et al. Quantitative analysis of total serum glycome in human and mouse. *Proteomics* 2016;16(21):2747–2758.

30. Furukawa J-I, et al. Impact of the Niemann-Pick c1 Gene Mutation on the Total Cellular Glycomics of CHO Cells. *J. Proteome Res.* 2017;16(8):2802–2810.

31. Gao C, et al. Sensitivity of heterozygous α1,6-fucosyltransferase knock-out mice to cigarette smoke-induced emphysema: implication of aberrant transforming growth factor-β signaling and matrix metalloproteinase gene expression. *J. Biol. Chem.* 2012;287(20):16699–16708.

32. Wang X, et al. Dysregulation of TGF-beta1 receptor activation leads to abnormal lung development and emphysema-like phenotype in core fucose-deficient mice. *Proc. Natl. Acad. Sci. U. S. A.* 2005;102(44):15791–15796.

33. Gonzalez DS, Jordan IK. The alpha-mannosidases: phylogeny and adaptive diversification. *Mol. Biol. Evol.* 2000;17(2):292–300.

34. Ross KA, et al. Comparison of Three Methods to Quantify Repair Cartilage Collagen Orientation. *Cartilage* 2013;4(2):111–120.

35. Glasson SS, et al. Deletion of active ADAMTS5 prevents cartilage degradation in a murine model of osteoarthritis. *Nature* 2005;434(7033):644–648.

536 36. Stanton H, et al. Investigating ADAMTS-mediated aggrecanolysis in mouse cartilage.
537 *Nat. Protoc.* 2011;6(3):388–404.

538 37. Estes BT, et al. Isolation of adipose-derived stem cells and their induction to a
539 chondrogenic phenotype. *Nat. Protoc.* 2010;5(7):1294–1311.

540 38. Patwari P, et al. Ultrastructural quantification of cell death after injurious compression
541 of bovine calf articular cartilage. *Osteoarthr. Cartil. OARS Osteoarthr. Res. Soc.*
542 2004;12(3):245–252.

543 39. Rao X, et al. An improvement of the 2ˆ(-delta delta CT) method for quantitative real-
544 time polymerase chain reaction data analysis. *Biostat. Bioinforma. Biomath.*
545 2013;3(3):71–85.

546 40. Ovchinnikov DA, et al. Col2a1-directed expression of Cre recombinase in
547 differentiating chondrocytes in transgenic mice. *Genes. N. Y. N 2000* 2000;26(2):145–
548 146.

549 41. Yamada T, et al. Carminerin contributes to chondrocyte calcification during
550 endochondral ossification. *Nat. Med.* 2006;12(6):665–670.

551 42. Nakamichi Y, et al. Chondromodulin I is a bone remodeling factor. *Mol. Cell. Biol.*
552 2003;23(2):636–644.

553 43. Lufkin T, et al. Homeotic transformation of the occipital bones of the skull by ectopic
554 expression of a homeobox gene. *Nature* 1992;359(6398):835–841.

555 44. Matsui Y, et al. Accelerated development of aging-associated and instability-induced
556 osteoarthritis in osteopontin-deficient mice. *Arthritis Rheum.* 2009;60(8):2362–2371.

557 45. Stoop R, et al. Type II collagen degradation in spontaneous osteoarthritis in C57Bl/6 and

558 BALB/c mice. *Arthritis Rheum.* 1999;42(11):2381–2389.

559 46. Fujitani N, et al. Qualitative and quantitative cellular glycomics of glycosphingolipids
560 based on rhodococcal endoglycosylceramidase-assisted glycan cleavage, glycoblotting-
561 assisted sample preparation, and matrix-assisted laser desorption ionization tandem
562 time-of-flight mass spectrometry analysis. *J. Biol. Chem.* 2011;286(48):41669–41679.

563 47. Takegawa Y, et al. Simultaneous analysis of heparan sulfate, chondroitin/dermatan
564 sulfates, and hyaluronan disaccharides by glycoblotting-assisted sample preparation
565 followed by single-step zwitter-ionic-hydrophilic interaction chromatography. *Anal.*
566 *Chem.* 2011;83(24):9443–9449.

567 48. Furukawa J, et al. Quantitative O-Glycomics by Microwave-Assisted β-Elimination in
568 the Presence of Pyrazolone Analogues. *Anal. Chem.* 2015;87(15):7524–7528.

569 49. Furukawa J, et al. Comprehensive approach to structural and functional glycomics based
570 on chemoselective glycoblotting and sequential tag conversion. *Anal. Chem.*
571 2008;80(4):1094–1101.

572

573 **FIGURES**

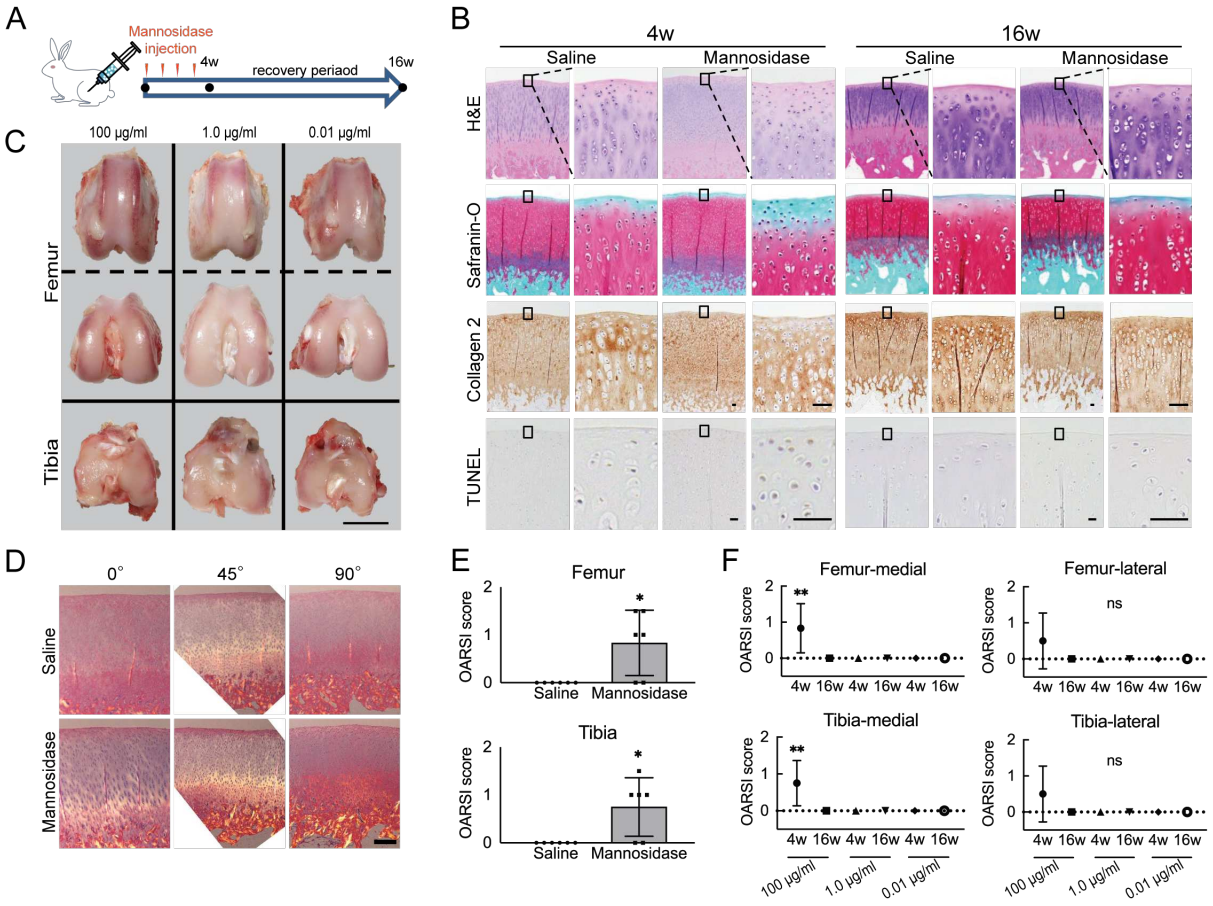

574

575 **Fig. 1. Effects of α-mannosidase injection in the knee joint in vivo.**

576 **(A)** Time course of intra-articular α-mannosidase injection and unloading. Red arrows
577 indicate the one-shot, intra-articular injection that was performed once a week. **(B)**
578 Histological evaluation of knee articular cartilage 4 weeks after intermittent α-mannosidase
579 infusion and 16 weeks after load removal. Scale bars, 50 μm. **(C)** Representative macroscopic
580 assessment of the articular cartilage using mannosidase concentration. Scale bar, 1 cm. **(D)**
581 Evaluation of the collagen orientation of reparative tissues at 4 weeks postoperatively.
582 Sections stained with HE was viewed under a polarized light microscope at multiple angles
583 (0°, 45°, and 90°). Scale bar, 200 μm. **(E)** OARSI scores at 4 weeks postoperatively on
584 sections from the knee joint (n = 6). **(F)** Tissue degeneration scores at each time point are
585 based on mannosidase concentration. Data are shown as mean ± standard deviation. **P* <

586 0.05, $^{**}P < 0.01$ versus the saline group in (E), and versus 4 weeks in (F). In (E), the Welch
587 t-test was used for statistical analysis. In (F), n = 6 rabbits per group. One-way analysis of
588 variance with Tukey's multiple comparison test was used to perform statistical analysis. HE,
589 hematoxylin and eosin; OARSI, Osteoarthritis Research Society International; TUNEL,
590 terminal deoxynucleotidyl transferase dUTP nick end labeling.

591

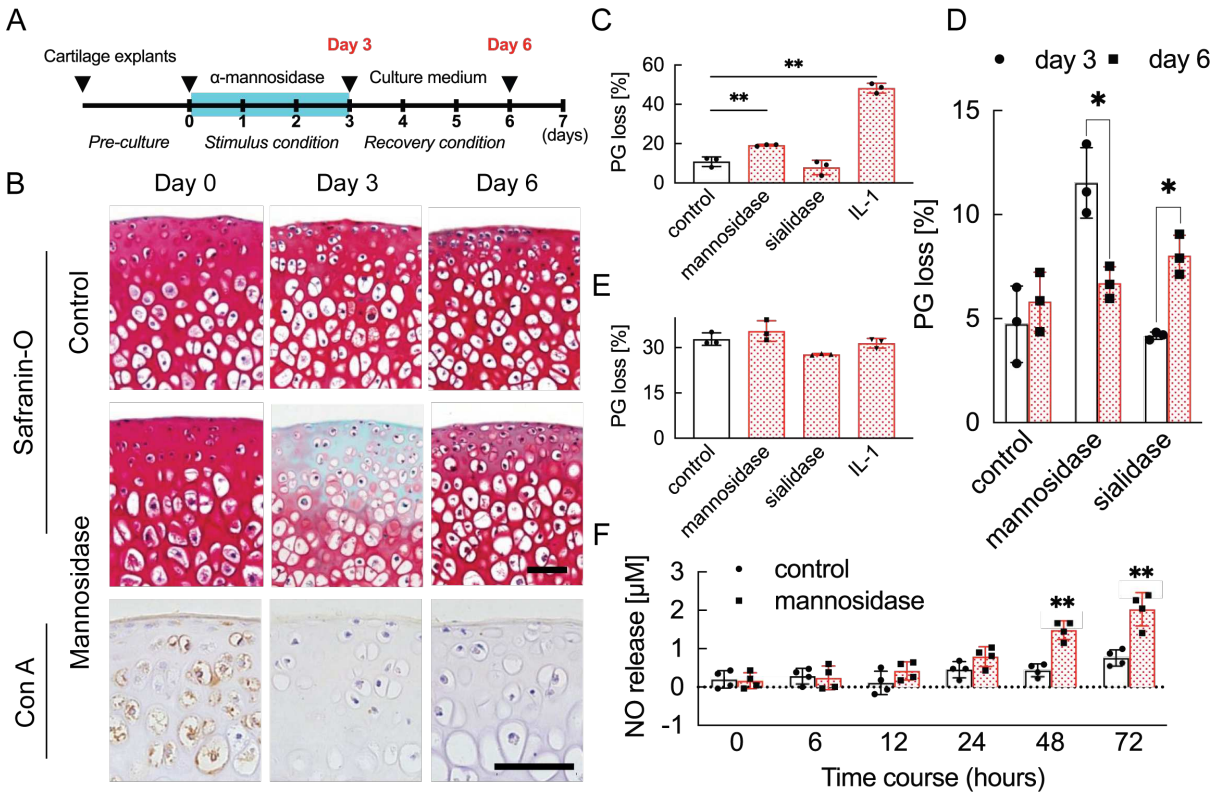

Fig. 2. Cartilage degradation induced by mannosidase stimulation.

(A) Schematic diagram of the procedures used to establish the early OA model before irreversible and progressive destruction of articular cartilage. (**B)** Mannosidase-treated cartilage stained with Safranin O and Con A. The distribution of high-mannose type N-glycans is decreased in mannosidase-induced degraded mouse cartilage. Scale bars, 50 μm. **(C), (D)** PG release after exposure to mannosidase (C) and recovery after its removal from cultured cartilage grafts (D). (**E)** To investigate the non-chondrocyte-mediated release of fragments, PG loss was measured in cartilage explants that had undergone freeze-thaw cycles. (**F)** Sequential NO released into media measured as concentrations of nitrite for cartilage explants stimulated with mannosidase. Data are shown as mean ± standard deviation (s.d.). $*P < 0.05$, $**P < 0.01$ versus the control group in **c**, **e,** and (F), and versus day 3 in (D). In (C) and (E), n = 3 samples (six mice) per group. One-way ANOVA with the Tukey multiple comparison test was used to perform statistical analysis. In (D), n = 12 mice in each group and n = 3 samples (six mice) at each time point. In (F), n = 16 mice at each time point

607 and n = 4 samples (eight mice) per group. In (D) and (F), two-way ANOVA with the Sidak

608 multiple-comparisons test was used to perform statistical analysis. Con A, concanavalin A;

609 NO, nitric oxide; ANOVA, analysis of variance; PG, proteoglycan.

610

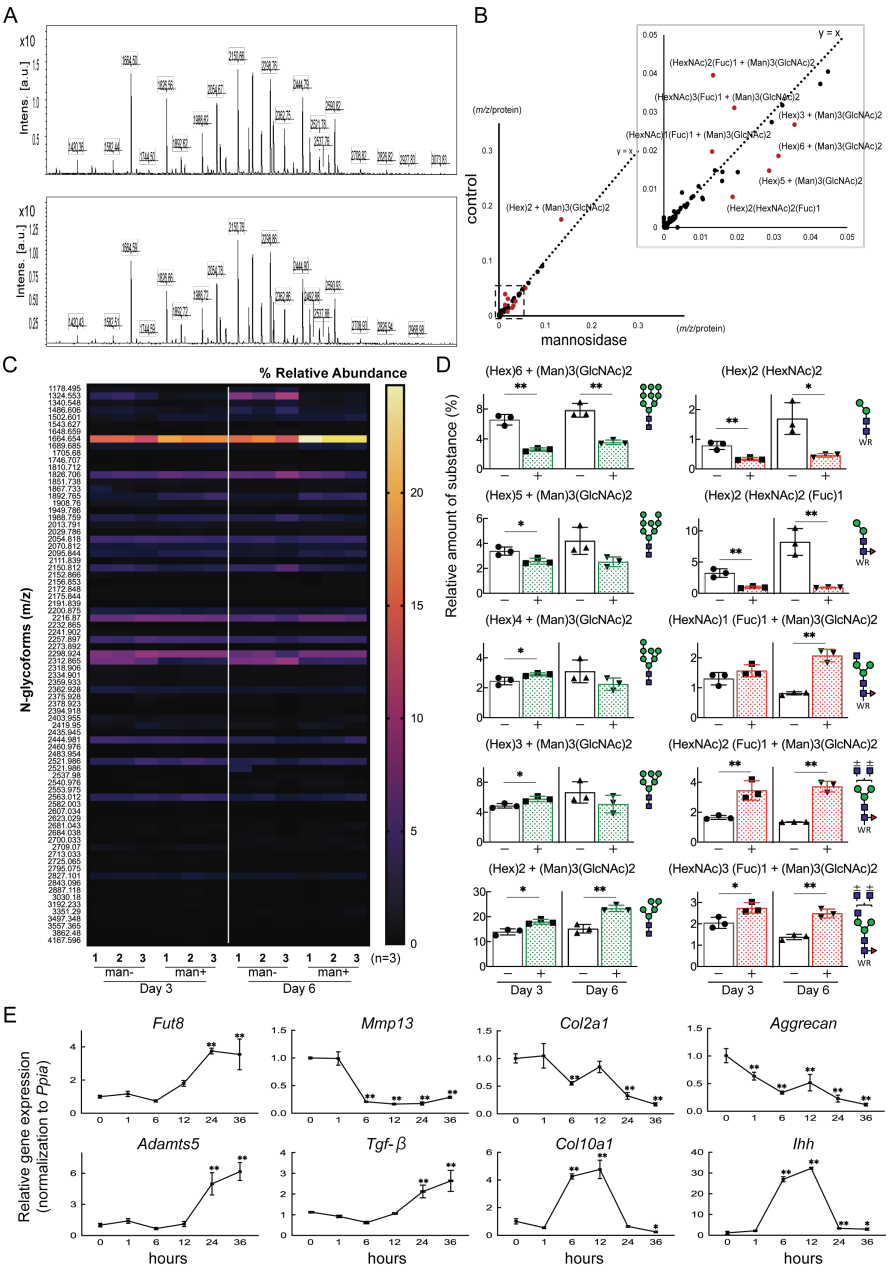

Fig. 3. Cartilage N-glycomes.

(A) MALDI-TOF MS spectra showing the quantitative N-glycan profiles of cartilage before (upper) and after (lower) mannosidase treatment. **(B)** Scatter plot of the changes in *m/z* per protein abundance in the mannosidase (x-axis) and control (y-axis) N-glycan structures. The red dots indicate the top 10 N-glycan structures based on the deviation from the y = x line. **(C)** Heatmap of N-glycome showing differential N-glycan expression in the mannosidase (man+) group versus the control (man-) group. **(D)** N-glycans altered by mannosidase were

619 corefucosylated glycans and high-mannose type N-glycans. (**E)** RT-PCR expression analysis
620 of marker genes in organ culture of cartilage with mannosidase. Data are shown as mean ±
621 standard deviation. *$P < 0.05$, **$P < 0.01$ versus the control group in (D), and versus 0 hours
622 in (E). In (D) and (E), n = 3 samples (six mice) per group. In (D), unpaired t-tests were used
623 to perform statistical analyses. In (E), one-way ANOVA with the Dunnett multiple
624 comparison test was used to perform statistical analysis. MALDI-TOF MS, matrix-assisted
625 laser desorption/ionization-time of flight mass spectrometry; ANOVA, analysis of variance;
626 RT-PCR, real-time polymerase chain reaction.

627

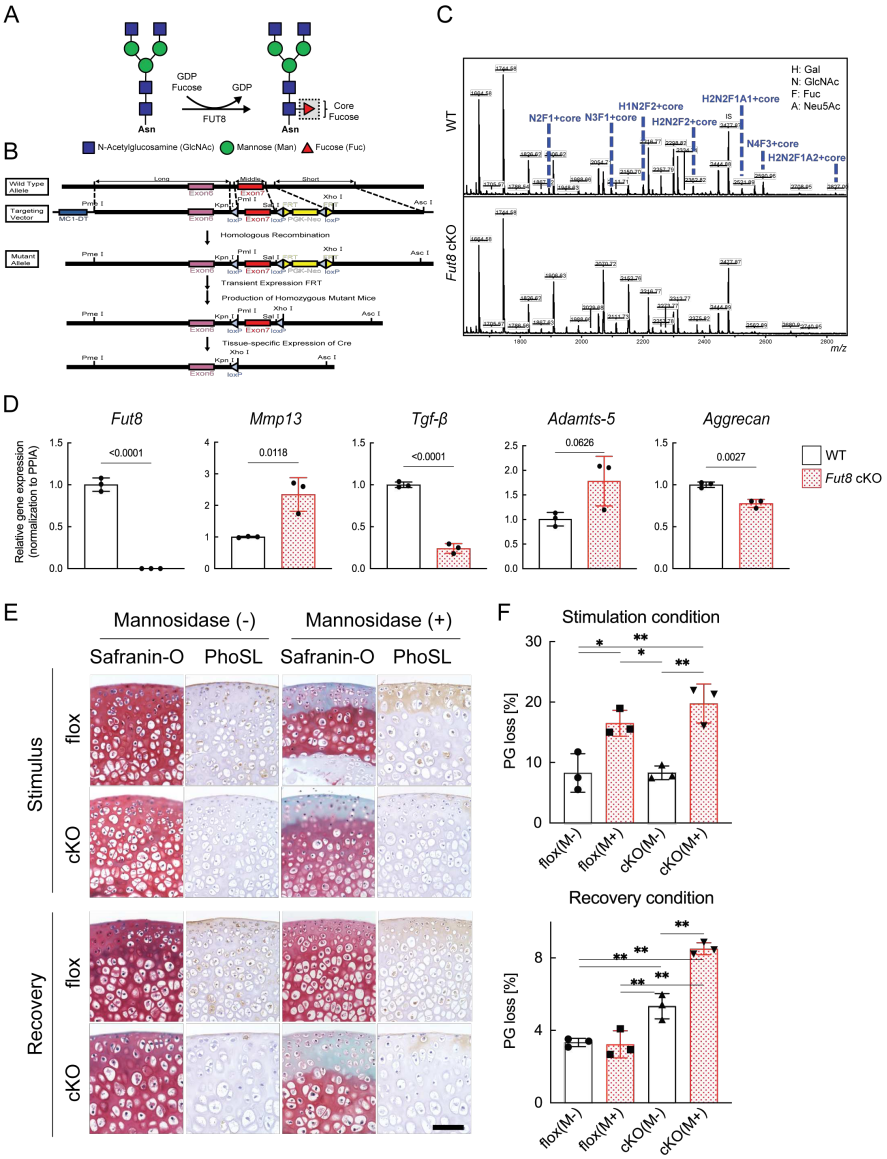

Fig. 4. Loss of resilience due to FUT8 deficiency in cartilage.

(A) Biological reaction of FUT8. FUT8 transfers fucose to the innermost GlcNAc residue of complex N-glycans via α1,6-linkage (corefucosylation). **(B)** Targeted disruption of *Fut8* locus. The *Fut8* gene (WT allele; top), targeting vector (middle), and disrupted *Fut8* locus (mutant allele; bottom). Schematic representation of the *Fut8*-targeting strategy and Cre-mediated recombination of the $Fut8^{loxP}$ allele. **(C)** MALDI-TOF MS mass spectra of N-glycans from WT and *Fut8* cKO mice. The corefucosylation levels in cartilage were

637 decreased and undetectable in *Fut8* cKO mice. (**D)** Gene profile in chondrocytes isolated
638 from *Fut8* cKO mice. The expression levels of these genes in WT cells were set to 1. PPIA,
639 peptidylprolyl isomerase A. (**E)** Histological findings in cartilage explants from *Fut8* cKO
640 mice and their floxed littermates, cultured with mannosidase and subjected to Safranin O
641 staining and PhoSL lectin staining. Scale bar, 50 μm. (**F)** PG release in cultured cartilage
642 explants from *Fut8* cKO mice and their floxed littermates. Data are shown as mean ±
643 standard deviation. In (E), n = 3 samples (six mice) per group. *$P < 0.05$, **$P < 0.01$ versus
644 the control group. One-way ANOVA, with the Tukey multiple comparison test, was used to
645 perform statistical analysis. MALDI-TOF MS, matrix-assisted laser desorption/ionization-
646 time of flight mass spectrometry; WT, wild-type; cKO, conditional knockout; PG,
647 proteoglycan; ANOVA, analysis of variance.

648

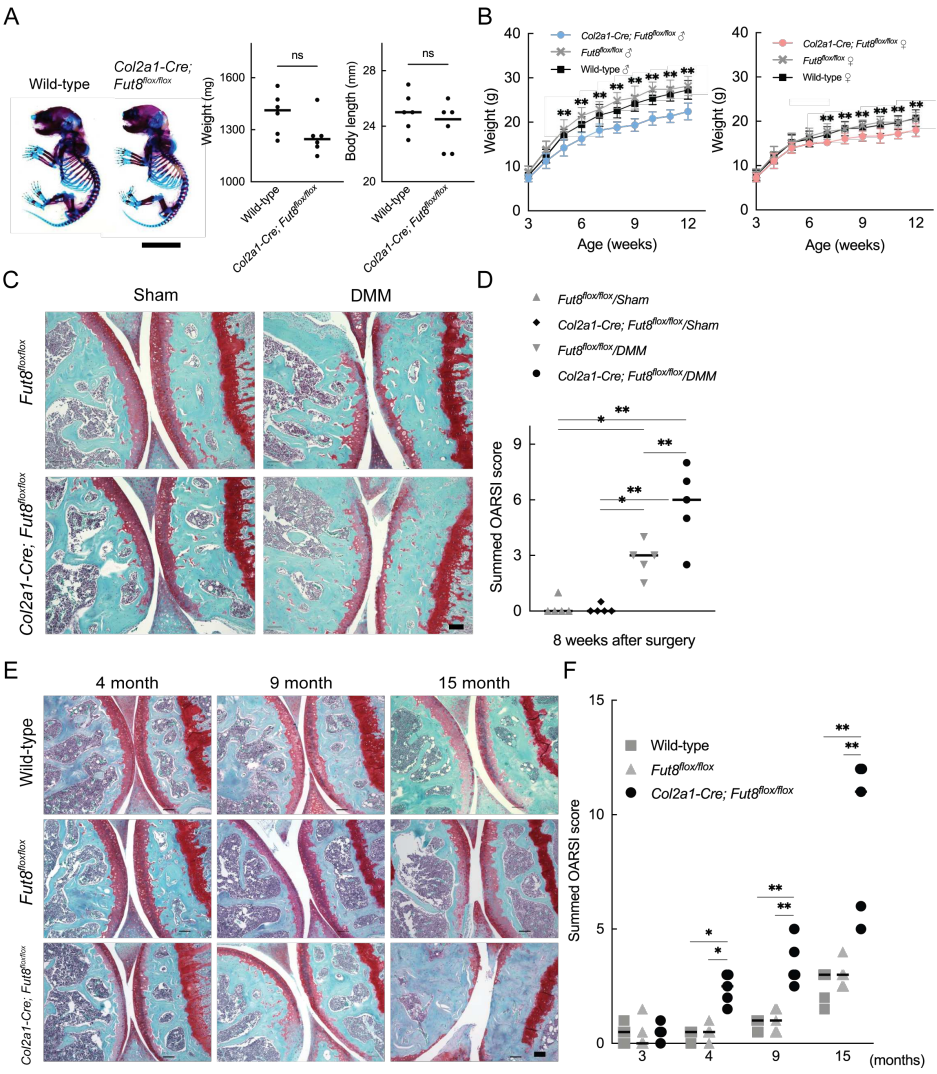

Fig. 5. OA acceleration in *Fut8* cKO mice.

(A) Double staining with alizarin red and alcian blue of the whole skeleton of wild-type and *Col2a1-Cre;Fut8*$^{flox/flox}$ cKO littermate embryos (newborn). Scale bars, 1 cm (left). Weight and body length of wild-type and cKO littermate embryos (right). **(B)** Growth curves determined by body weight in male (left) and female (right) wild-type mice and their cKO littermates. **(C)**, **(D)** Features of instability-induced OA in *Fut8*$^{flox/flox}$ (flox) mice and their cKO littermates at 8 weeks after surgery. Safranin O staining is shown for each mouse genotype. Scale bar, 100 μm (C). Summed histological scores for OA severity in the knee cartilage from flox and cKO mice, as determined using the OARSI scoring system, are shown (D). **(E)**, **(F)** Features of age-associated osteoarthritis in wild-type mice and their flox and

cKO littermates. Safranin O staining of the knee joint is shown for each mouse genotype at 3, 4, 9, and 15 months of age. Scale bar, 100 μm (E). The summed OARSI scores are shown (F). Data are shown as mean ± standard deviation. In (A), the Welch t-test was used to perform statistical analyses (n = 6 mice per group). In (B), n = 15 mice per group at each time point. In (D) and (F), n = 5 mice per group at each time point. *$P < 0.05$, **$P < 0.01$ versus the wild-type group in (B) and (F), and versus flox mice in (D). One-way ANOVA with the Tukey multiple comparisons test (B), (D) and two-way ANOVA with the Tukey multiple comparisons test (F) were used to perform statistical analysis. OA, osteoarthritis; cKO, conditional knockout; OARSI, Osteoarthritis Research Society International. ANOVA, analysis of variance; ns, not significant.

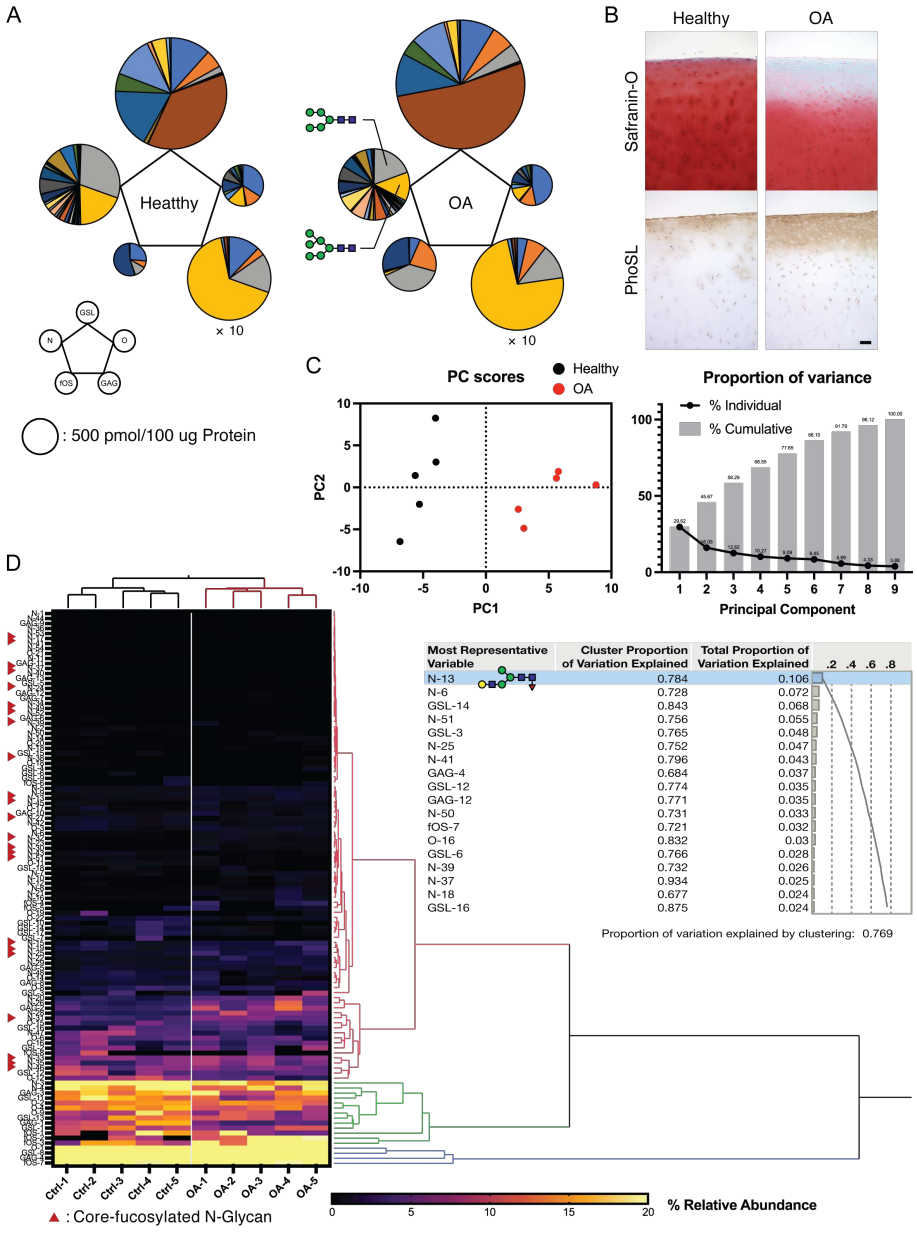

Fig. 6. Altered glycosylation of human Osteoarthritis (OA) cartilage based on comprehensive glycan analysis.

(A) Total glycome profiling of human OA cartilage. Pie charts at the vertices of the pentagon correspond to the glycan expression profiles of N-glycans, O-glycans, GSL-glycans, free oligosaccharides (fOS), and glycosaminoglycan (GAG). The size of each circle and its constituent colors reflect the absolute quantity of glycans (pmol/100 μg protein) and the glycan substructures, respectively. The sizes of the circles representing the GAG contents are increased by 10-fold. Each color indicates the estimated glycan structure and corresponds to

680 the respective glycan number listed in the S3 Table. (**B)** Expression of core fucose in healthy
681 and OA cartilage. Scale bar, 100 μm. (**C)** Principal component analysis (PCA) of a glycan
682 expression data set. Data points represent individual samples. The first principal component
683 (PC1) distinguishes healthy and OA samples. (**D)** Hierarchical cluster analysis results
684 showing cluster image display for total glycans with color gradient for relative glycan
685 expression and dendrogram for each glycan structure. Cluster summary of PCA on the
686 glycome are shown on the right. The most representative variable is (Hex)1 (HexNAc)1
687 (Fuc)1 + (Man)3(GlcNAc)2 that means the largest squared correlation with its cluster
688 component.
689
690